

An Approach to Fault Diagnosis of Rolling Bearings

A. A. Roque^{*,**}, T. A. N. Silva^{*}, J. M. F. Calado^{*,§} and J. C. Q. Dias^{*,§§}

^{*} ISEL - Instituto Superior de Engenharia de Lisboa
Polytechnic Institute of Lisbon, Mechanical Engineering Department
Rua Conselheiro Emídio Navarro, 1959-007 Lisboa, Portugal

[§] IDMEC - Institute of Mechanical Engineering
Instituto Superior Técnico, Technical University of Lisbon,
Av^a Rovisco Pais 1049-001- Lisboa, Portugal

^{§§} CENTEC - Centre of Marine Technology and Engineering
Instituto Superior Técnico, Technical University of Lisbon
Av^a Rovisco Pais 1049-001- Lisboa, Portugal

^{**} DatAnálise, Serviços e Técnicas de Manutenção, Lda.
Rua João Teixeira Simões, 2, 1^o andar, 2780-254 Oeiras, PORTUGAL
aroque@datanalise.pt, {tasilva, jcalado, jdias}@dem.isel.ipl.pt

Abstract: - The present paper aims to demonstrate why usually when theoretical mathematical models are used to compute the frequencies corresponding to a faulty rolling bearing a deviation is obtained between the computed values and the real frequencies emitted by such a device. A laboratory rolling bearing test ring has been developed to perform the current studies. From the obtained results we highlight the impact of the cage rotation frequency on the referred deviation of measured values from the theoretical ones.

Key-Words: Fault detection, Fault isolation, Fault diagnosis, Rolling bearing, Condition based maintenance.

Notation

$\omega_{i,g,e,r}$ - Angular speed of inner race, cage, outer race and rolling element;

$V_{i,g,e,r}$ - Linear speed of inner race, cage, outer race and rolling element;

$r_{i,g,e,r}$ - Radius of inner race, cage, outer race and rolling element;

$f_{i,g,e,r}$ - Rotation frequency of inner race, cage, outer race and rolling element;

d - Diameter of the rolling element;

$D_{i,e,P}$ - Diameter of inner race, outer race and pitch;

θ - Contact angle;

N - Number of rolling elements.

1 Introduction

The maintenance area is an example that offers challenges to both science and companies in order to optimize the performance of equipment and facilities [1]. Therefore, there is a need from industry to have an economy and efficient machine fault diagnostic system. The occurrence of a fault must be identified as early as possible to avoid fatal breakdown of machines [2]. Hence, it is possible to increase the reliability of the system so as to

rationalize costs, by developing new management models and new algorithms based on on-line monitoring of several parameters, namely vibrations, electrical variables, temperature, among others [3].

The bearing is a central component in the most part and types of rotary machines and its reliability defines the reliability and quality requirements of the machine as whole. Therefore, a rolling bearing fault represents an undesirable and baleful occurrence.

Thus, first of all, a good product design is essential to achieve products with high reliability, quality and performance [4].

Second and more recently, in order to realize near-zero downtime and maximum productivity, proactive maintenance, which needs advanced tools of prognostics, has received more and more attention [5].

Similarly, the most traditional condition based maintenance philosophy of using vibration information to lower operating costs and increase machinery availability is gaining acceptance throughout industry, being now used as a complement of proactive maintenance.

Since most of the machinery in a condition maintenance program contains rolling element bearings, it is imperative to establish a suitable

condition monitoring procedure to prevent malfunction and breakage during operation [6-8]. However, the first time someone try to approach the rolling bearing fault detection and isolation topic several difficulties arise. Often such difficulties last for years until the degradation process has been well understood and mainly the signal processing methodology, the fault detection procedure and the reason to achieve deviations between the frequencies evaluated through the theoretical model and the frequencies emitted by the rolling bearing.

Vibration signals emitted by a faulty rolling bearing usually include frequencies related to its geometry, fault location and rotation speed of inner and outer races.

This paper presents a didactic study based on lab equipment developed to test and analyse faulty rolling bearings. Findings from this small-scale study indicate a strong relationship between the work task goal and the level of relevance used for judging resources during search processes [9]. In this case has been promoted the comparison between several vibration signals emitted by faulty rolling bearings, which has enabled to achieve a deeper understanding of how the corresponding fault detection and isolation is performed in practice. The paper's aim is to identify the factors responsible for the deviations achieved between the theoretical mathematical models and the real frequencies emitted by a faulty rolling bearing. Thus, the paper is organised as follows: Section 2 provides a description of the theoretical mathematical models usually used to compute the values of frequencies emitted by a faulty rolling bearing; Section 3 reviews the fault detection and diagnosis techniques usually applied for faulty rolling bearings; Section 4 presents a case study, including a lab ring description; Section 5 provides a description of tests performed together with a results discussion; Section 6 presents some concluding remarks.

2 Theoretical Mathematical Models

A faulty rolling bearing usually emit the following main frequencies:

FTF - (*Fundamental Train Frequency*) – frequency emitted by a faulty cage;

BPFO – (*Ball Pass Frequency of the Outer Race*) – frequency emitted by a rolling element bearing when it impacts a superficial defect in the outer race;

BPFI – (*Ball Pass Frequency of the Inner Race*) – frequency emitted by a rolling element bearing

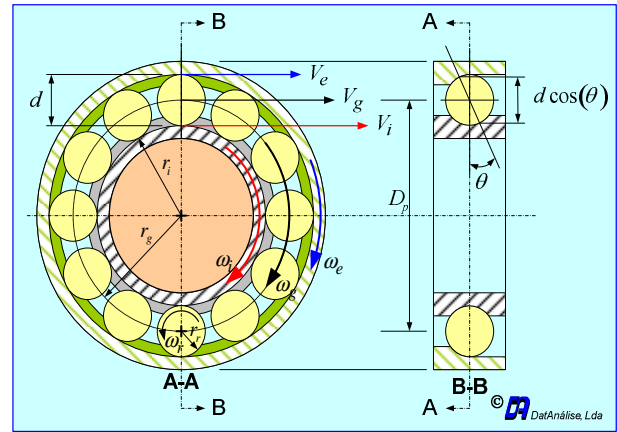


Fig. 1. Rolling bearing geometry.

when it impacts a superficial defect in the inner race;

BSF – (*Ball Spin Frequency*) – frequency emitted when a rolling element bearing with a superficial defect impacts the inner or outer races.

The frequency spectrum of a faulty rolling bearing includes not only the inner and outer races rotation frequencies but also the harmonics corresponding to the fault frequency and sidebands as a result of the amplitude modulation. Such sidebands are related to the values of the cage frequency rotation or to the inner or outer race frequency rotation.

A faulty rolling bearing produces certain frequencies depending on rolling element bearing geometry, which is shown in Figures 1 and 2, number of rolling elements and shaft speed. The cage angular speed is given as follows:

$$\omega_g = \frac{V_g}{r_g} \tag{1}$$

The outer race angular speed is given by equation (2),

$$\omega_o = \frac{V_o}{r_o} \tag{2}$$

and the inner race angular speed is given as follows,

$$\omega_i = \frac{V_i}{r_i} \tag{3}$$

Considering there is no sliding between the rotating parts, the cage linear speed can be given by,

$$V_g = \frac{V_i + V_o}{2} = \frac{\omega_i r_i + \omega_o r_o}{2} \tag{4}$$

Analysing Fig. 2 the following can be achieved,

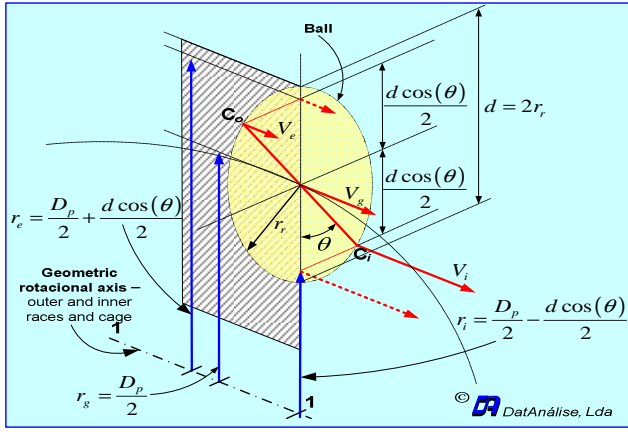


Fig. 2. Rolling bearing geometry - contact angle θ .

$$r_g = \frac{D_p}{2} \quad (5)$$

$$r_i = \frac{D_p}{2} - \frac{d \cos(\theta)}{2} \quad (6)$$

$$r_e = \frac{D_p}{2} + \frac{d \cos(\theta)}{2} \quad (7)$$

$$r_r = \frac{d}{2} \quad (8)$$

Putting all the results together, the cage angular speed can be given as follows,

$$\omega_g = \frac{1}{2} \left[\omega_i \left(1 - \frac{d \cos \theta}{D_p} \right) + \omega_e \left(1 + \frac{d \cos \theta}{D_p} \right) \right] \quad (9)$$

Being $\omega_g = 2\pi f_g$ equation (9) gives de value for FTF, which can be expressed in [Hz] as follows,

$$FTF = f_g = \frac{1}{2} \left[f_i \left(1 - \frac{d \cos \theta}{D_p} \right) + f_e \left(1 + \frac{d \cos \theta}{D_p} \right) \right] \quad (10)$$

By other words, equation (10) provides the cage rotation frequency, which when appears in the frequency spectrum is related with the unbalanced of rotating elements – cage and rolling elements due to cage wear or looseness development. Its appearance can also be related to amplitude modulated due to defects in the inner and outer races. The defect frequency called above BPFO can be evaluated multiplying the number of rolling elements by the relative angular speed between cage and outer race. Thus, BPFO can be given as,

$$BPFO = N (\omega_g - \omega_e) \quad (11)$$

Putting equation (9) into (11) the following is obtained,

$$BPFO = N \left\{ \frac{1}{2} \left[f_i \left(1 - \frac{d \cos \theta}{D_p} \right) + f_e \left(1 + \frac{d \cos \theta}{D_p} \right) \right] - f_e \right\} \quad (12)$$

Through mathematical manipulation equation (12) can be written as follows,

$$BPFO = \frac{N}{2} (f_i - f_e) \left(1 - \frac{d \cos \theta}{D_p} \right) \quad (13)$$

In a similar way the defect frequency quoted above as BPFi can be evaluated multiplying the number of rolling elements by the relative angular speed between cage and inner race, being given as follows,

$$BPFi = N (\omega_i - \omega_g) \quad (14)$$

Putting equation (9) into (14) and doing some simplifications the following formula is achieved to evaluate BPFi,

$$BPFi = \frac{N}{2} (f_i - f_e) \left[1 + \left(\frac{d \cos \theta}{D_p} \right) \right] \quad (15)$$

The defect frequency called above as BSF can be defined as the rolling element frequency rotation, ball or roller, by its own centre. The ball or roller angular speed in turn its own centre is given as follows,

$$\omega_r = \frac{V_r}{r_r} \quad (16)$$

Considering that only a pure rotation exists and there is no sliding, the ball or roller tangential speed in the contact point with the inner race is given by the following formula,

$$V_r = (\omega_i - \omega_g) r_i \quad (17)$$

Putting the equation (17) into (16) the following equation is obtained,

$$\omega_r = \frac{(\omega_i - \omega_g) r_i}{r_r} \quad (18)$$

Putting equations (6), (8) and (9) into equation (18) the following equation is achieve to evaluate the defect frequency BSF,

$$BSF = f_r = \frac{D_p}{2d} (f_i - f_e) \left[1 - \left(\frac{d \cos \theta}{D_p} \right)^2 \right] \quad (19)$$

In the case where the rolling elements are rollers is usually the appearance of the frequency $2 \times \text{BSF}$ since impulses are emitted when the defect contacts the inner and outer races during one roller rotation. When a defect is formed on one of the rolling bearing parts mentioned above, related frequency, its orders, its sidebands, etc. may arise in the spectrum plot. The overall mathematical model presented so far, allowing evaluating the defects frequencies, is general since has been considered not only the inner race rotation speed but also the outer race rotation speed. However, in most of the practical situations the outer race is stationary and the mathematical model presented above can be simplified.

2.1 Simplified mathematical model

Therefore, when the outer race is considered stationary the mathematical model to compute the values for the defect frequencies can be written as follows,

$$\begin{aligned} FTF &= \frac{1}{2}(f_i) \left(1 - \frac{d \cos \theta}{D_p} \right) \\ BPF O &= \frac{N}{2}(f_i) \left(1 - \frac{d \cos \theta}{D_p} \right) \\ BPF I &= \frac{N}{2}(f_i) \left(1 + \frac{d \cos \theta}{D_p} \right) \\ BSF &= \frac{D_p}{2d}(f_i) \left[1 - \left(\frac{d \cos \theta}{D_p} \right)^2 \right] \end{aligned} \quad (20)$$

Comparing the above equations (20), the following relationships between them can be written,

$$\begin{aligned} BPF O &= N (FTF) \\ BPF I &= N (f_i - FTF) \end{aligned} \quad (21)$$

Therefore, to compute the values of the defect frequencies is compulsory to know the geometric rolling bearing characteristics. When such characteristics are unknown the use of approximate equations is possible as presented in the following sub section.

2.2 Empirical mathematical model

When the contact angle is unknown but the remaining parameters are known, the mathematical model (20) can be used doing $\theta = 0$. If in extreme cases the number of parameters known not allows the use of the mathematical model (20),

alternatively, the following equations, which have been achieved empirically, can be used to compute approximated values for the frequencies emitted by a faulty rolling bearing,

$$\begin{aligned} FTF &= 0.4 f_i \\ BPF O &= 0.4 N f_i \\ BPF I &= 0.6 N f_i \end{aligned} \quad (22)$$

The empirical mathematical model (22) is based on the fact that in a complete rotation of the inner race, about 40% of the rolling elements contact a defect in the outer race and 60% of the rolling elements contact a defect in the inner race [10].

3 Fault Detection/Isolation Techniques

In the past several decades, many different techniques have been developed to condition based maintenance for monitoring and diagnosis rolling element bearings. Some detailed reviews of such techniques can be found in [8,11]. Among them, vibration and acoustic emission (AE) signals are widely used in condition monitoring of rotating machine. However, from those techniques, visual inspection of time-domain or frequency-domain features of the measured vibration signals has long been performed [12].

3.1 Time-domain / Trend Curves

Time domain methods usually involve indices that are sensitive to impulsive oscillations, such as peak level, root mean square (RMS) value, crest factor (peak/RMS) analysis, kurtosis analysis, shock pulse counting, time series averaging method, signal enveloping method and many more [13,14]. A healthy (no faulty) rolling bearing usually produces a vibration signature with Gaussian distribution [15].

Generally, this type of measurement gives limited information but can be useful when used for trending, where an increasing vibration level is an indicator of a deteriorating rolling bearing condition.

Trend analysis involves plotting the vibration level as a function of time and using this to predict when the rolling bearing must be taken out of service for repair. Another way of using the measurement is to compare the levels with published vibration criteria for different types of equipment.

Detection generally uses the most basic form of vibration measurement, where the overall vibration

level is measured on a broadband basis in a range for example, 10-1,000Hz or 10-10,000Hz. In rolling bearings where there is little vibration, the vibration signal indicated by the Crest Factor may imply incipient defects, whereas the high energy level given by the RMS level may indicate severe defects. Although broadband vibration measurements may provide a good starting point for fault detection it has limited diagnostic capabilities and although a fault may be identified it may not give a reliable indication of where the fault is, i.e. rolling bearing deterioration/damage, unbalance, misalignment, and so on.

When an improved diagnostic capability is required, frequency analysis is normally used, which usually gives a much earlier indication of the development of a fault and also the source of the fault, as will be described in the next sub-section.

3.2 Frequency domain

Frequency analysis plays an important part in the detection and isolation of rolling bearing faults. In the time domain the individual contributions to the overall machine vibration are difficult to identify. In the frequency domain they become much easier to identify and can therefore be easily related to individual sources of vibration. Time domain methods only allow rolling bearing fault detection while frequency domain methods allow detecting, isolating and characterizing faults, which is called diagnosis.

Frequency domain analysis or spectral analysis using the Fast Fourier Transform (FFT) is probably the most used technique for rolling bearing fault detection and isolation.

The rolling elements experience some slippage as the rolling elements enter and leave the bearing load zone. As a consequence, the occurrence of the impacts never reproduces exactly at the same position from one cycle to another. Moreover, when the position of the defect is moving with respect to the load distribution of the rolling bearing, the series of impulses is modulated in amplitude. However, the periodicity and the amplitude of the impulses experience a certain degree of randomness. In such case, the signal is not strictly periodic, but can be considered as cyclo-stationary (periodically time-varying statistics). All these make the rolling bearing defects very difficult to detect and diagnosed by conventional FFT-spectrum analysis which assumes that the analyzed signal is strictly periodic. Thus, a method of conditioning the signal, before the spectrum estimation has been performed, is needed.

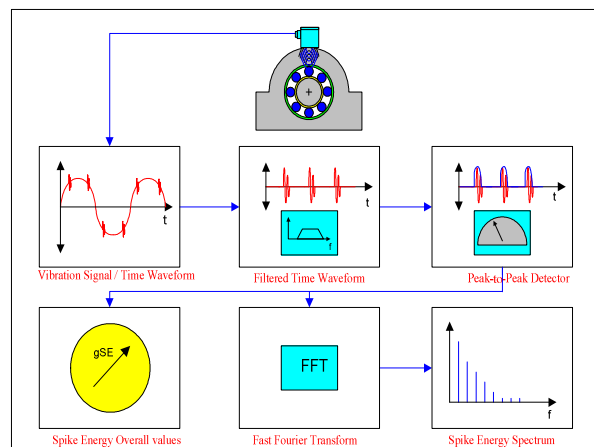


Fig. 3. Spike Energy signal processing.

To overcome the modulation problem, several signal envelope demodulation techniques have been introduced. One of the most popular is the high-frequency resonance technique (HFRT), where an envelope detector demodulates the band pass filtered signal and the frequency spectrum is determined by FFT technique [15]. A particular case of this technique is the so called Spike Energy Spectrum where the measured magnitude of the signal is expressed in “gSE” units (acceleration units of Spike Energy) [16].

Spike Energy spectrum and Spike Energy time waveform were developed and used in recent years in fault detection and isolation analysis. Following such technique the vibration signal is measured by an accelerometer and filtered by frequency band pass filters or high pass filters. The purpose of using high pass corner frequencies is to reject low-frequency vibration signals, such as unbalance, misalignment and looseness. Then, the filtered signal passes through a peak-to-peak detector, which not only holds the peak-to-peak amplitude but also applies a carefully selected decay time constant.

The decay time constant is directly related to the spectrum maximum frequency (F_{max}). The output signal from Spike Energy peak-to-peak detector is a saw-tooth shape signal. This saw-tooth shape signal is further processed to calculate Spike Energy overall magnitude and Spike Energy spectrum by using the FFT. Signal processing for Spike Energy analysis is schematic represented in Figure 3.

The peak-to-peak detector is unique and very sensitive to the defect frequency as compared to other envelope detection or demodulation method. In an envelope detection, the vibration signal is first passed through a high pass (or band pass) filter. The filtered signal is full wave (or half wave) rectified. Then, the rectified signal is passed

through a low pass filter to separate the modulation (or defect) frequency from the carrier frequency.

The low-pass filtering has an averaging effect on the rectified signal and the peaks are smoothed in the demodulated waveform. In contrast, Spike Energy detection preserves the severity of defects by holding the peak-to-peak amplitude of the impulses. It also enhances the fundamental defect frequency and its harmonics by applying a proper selected decay time constant.

3.3 Other techniques

Normal and damage rolling bearings vibrate when rotate. There has been much research on the vibration measurement analysis of rolling bearings which have damages on the raceway surface, showing that such measurements are useful for rolling bearing fault diagnosis.

More recently, some authors have pointed out that the measurement of time intervals of Acoustic Emission (AE) for rolling bearings can also be useful for the same purpose if the AE occurred at normal and faulty bearings during operation.

Furthermore, as AE refers to the generation of transient elastic waves produced by a sudden redistribution of stress in material, some authors argue that AE has the advantage to be able to detect the accumulation of micro damage inside components, especially under service conditions [15]. Thus, such a technique allows detecting and isolating faults when they are in very incipient stage.

From what is written above can be concluded that there are two important phases to implement in the rotary parts faults detection and isolation: the first consists of performing a signal processing, in order to extract the typical features or “patterns” and diminish the signal noise, and the second phase consists of the signal classification based on the characteristics obtained in the previous step; these tasks are not direct for every type of signal, since, to manage them with relative success, some knowledge and experience in the field is needed [17].

Other techniques have been pointed out, as for instance, methods for fault diagnosis of rolling bearings using adaptive filtering techniques and fuzzy neural networks. The adaptive filtering could be used for noise cancelling and feature extraction from vibration signal measured for the diagnosis. Fuzzy neural networks could be used to automatically distinguish the fault types of a bearing by time domain features. Using the signals processed by adaptive filtering, the neural network can quickly converge when learning, and can

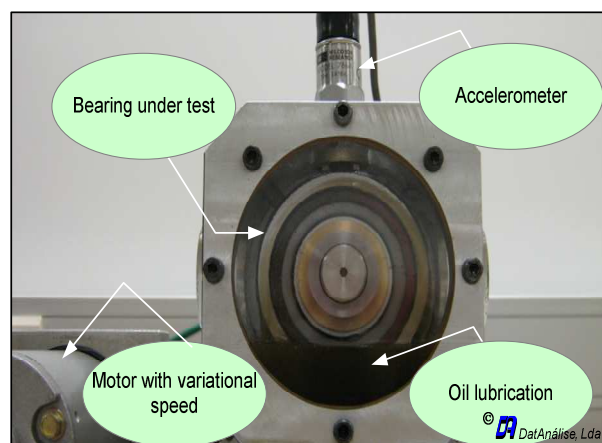


Fig. 4. Rolling bearing test ring.

quickly distinguish fault types when diagnosing [18].

Table 1. Rolling Bearing Parameters.

General characteristics of bearing NU 307 ECP			
Inner race diameter	46,2 mm		
Rolling element diameter	12,0 mm		
Outer race diameter	70,2 mm		
Primitive diameter	58,2 mm		
N° of rolling elements	12		
Contact angle	0°		
Inner diameter	35 mm		
Outer diameter	80 mm		
Dynamic load	64400 N	Reference speed (oil)	9500 rpm
Static load	63000 N	Limiting speed	2000 rpm
Radial clearance	25 a 50 µm	EC - Single row cylindrical roller bearing	
Minimum radial load	338 N	P - Injection moulded cage of glass fibre reinforced polyamide	

4 Rolling Bearing Test Ring

A laboratory rolling bearing test ring (Figure 4) has been developed and previously presented in [19]. Such a device allows shaft speed rotation changes and consequently variations of the rotational speed of the rolling elements of the bearing under test. On the other hand, we could apply distinguish radial loads over the outer race of the rolling bearing. The cage rotational speed is measured through a stroboscopic lamp.

In a future configuration we hope to measure applied loads and rotational speeds of the rolling elements by means of force cells and proximity sensors, respectively. The inner race rotates at the same speed of the shaft and has been measured using a laser photoelectric cell.

The characteristics of the four rolling bearings used during the current studies are summarized in

Table 1. In order to test four single fault types four equal rolling bearings have been used and a different single fault has been introduced in each one. The four fault types considered are single superficial defects on the following rolling elements:

- (i) inner race;
- (ii) outer race;
- (iii) roller;
- (iv) and cage.

A data acquisition system has been used to perform online acquisition and measurements. Acquired data such as global values, frequency spectrums in mm/s and gSE (envelope analysis), time signals in mm/s and g's (envelope analysis) and the shaft rotation speed (inner race speed) was analysed.

5 Tests

The present section summarizes the obtained results taken from the acquired data. Hence, typical results for each specific fault type are discussed, on a didactical point of view.

In current study the developed laboratory test rig, described on the previous section, has been used. As acquisition system an online system, Enwatch from Rockwell Automation, Inc., which receives vibration data from a piezoelectric accelerometer with integrated electronics from Wilcoxon Research, Inc., more precisely, Model 786A with 100mV/g, has been used. As parameters for the Spike Energy method the frequency band pass filter has been fixed with 5 kHz and 60 kHz, as low and high filter limits respectively. Data has been collected for a maximum frequency of 30 kCPM (cycles per minute) and 800 lines with a handing window.

6 Results and Discussion

First, with a previously introduced slight defect on the inner race, the envelope spectrum of Figure 5 has been obtained, on which the defect frequency of inner race (BPFI) and its harmonics can be seen, as well as each harmonic sidebands. Note that between sidebands a distance equal to the inner race rotation frequency can be observed. Such sidebands are due to the fact that the inner race is rotating and, thus, the defect will enter and leave the load zone causing a variation in the rolling element raceway contact force, hence deflections. While in the load zone, the amplitudes of the impacts will be highest, they are reduced as the

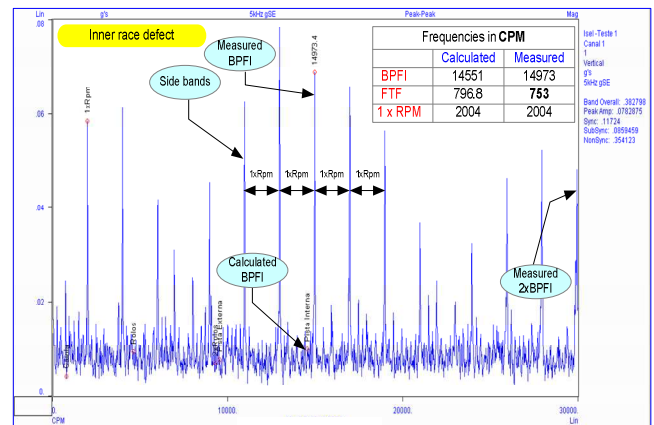


Fig. 5. Envelope spectrum - defect BPFI.

defect leaves the load zone. Such behaviour results in a signal where the defect frequency is modulated (amplitude-modulation) at inner race rotational frequency (shaft rotational speed). The corresponding time signal, depicted in Figure 6, shows the impacts occurring in the rolling bearing. The time between the highest peaks corresponds to the inner race rotation.

The analysis of the second fault type, outer race defect, can be observed through the envelope spectrum of Figure 7. Through the referred figure can be easily verified that each fault type has typical frequency plots, which can be used as support to a diagnosis decision. Getting back to Figure 7, the defect frequency of outer race (BPFO) and its harmonics have been identified. In this particular case, there appear no sidebands of the defect. This finding happens due to the fixation type of the bearing to the test apparatus, on which the outer race has a rigid constrain and, therefore, there is no amplitude-modulation. However, on some rolling bearing types the outer race has rotational motion and for those cases the defect frequency of outer race and its harmonics appear in the envelope spectrum modulated by the outer race rotational speed.

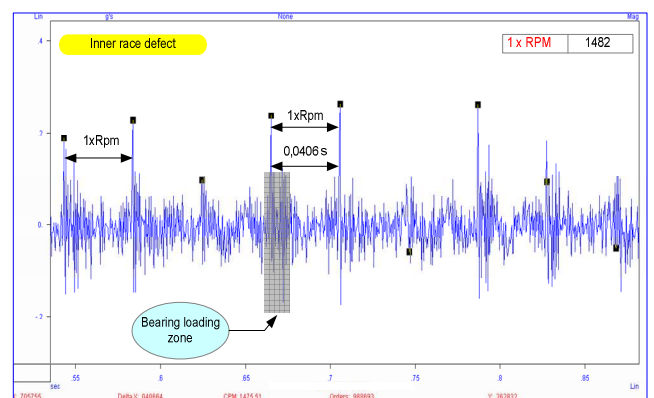


Fig. 6. Time signal in g's - defect BPFI

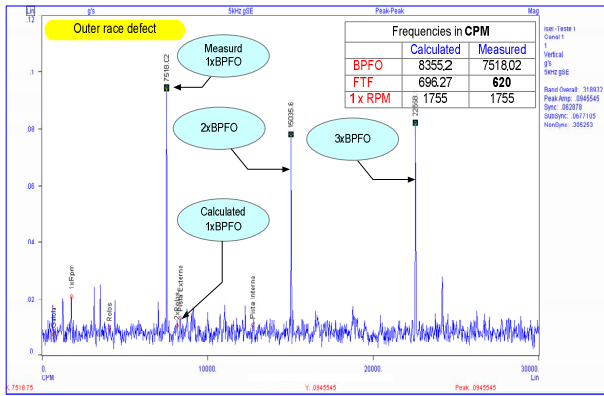


Fig. 7. Envelope spectrum - defect BPFO.

Dealing with the third fault type, roller defect, another type of frequency spectrums has been observed. Figure 8 has been achieved during experiments conducted with a rolling bearing with a faulty roller. It can be seen the fundamental defect frequency for the roller (BSF) and its harmonics, presenting sidebands at rotation frequency of the cage (FTF) due to amplitude-modulation.

Note that, for defects on the outer race and on the roller, the values measured for the fundamental defect frequencies are below the theoretical/calculated ones. However, for defects on the inner race, the previous statement is not true. In this case, the measured values corresponding to the defect frequencies are above the values achieved using the theoretical models presented in previous sections.

The last fault type considered, an isolated cage defect, does not occur very often in practice. Usually, the cage defect frequency (FTF) arises associated with other defects, such as those in the inner and outer races or rollers, which can be observed, e.g., in the spectrum achieved to the tested rolling bearing with a faulty roller element (Figure 9).

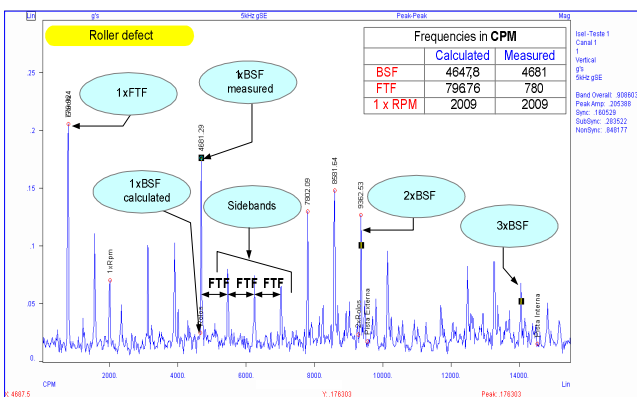


Fig. 8. Envelope spectrum - defect BSF.

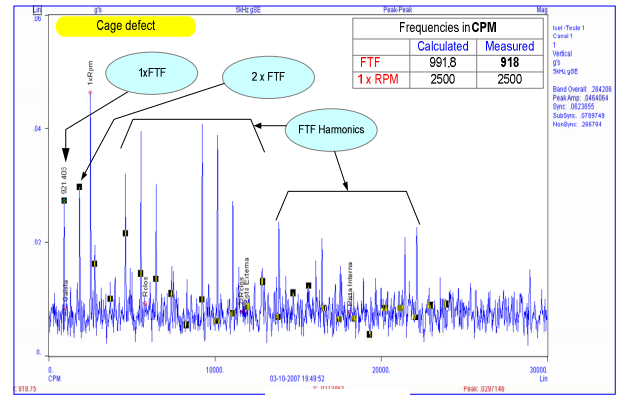


Fig. 9. Envelope spectrum - defect FTF.

Such damage mechanism can be observed as an unbalanced of rotating elements (cage, balls or rollers). During the current studies, such a defect has been simulated in a rolling bearing by extracting one roller. The spectrum depicted in Figure 9 presents the defect frequency of the cage (FTF) and respective harmonics. In the case of a cage defect, and due to its relationship with an unbalanced, its effect is more visible in a frequency spectrum in mm/s as could be observed in Figure 10. Such damage mechanism can be observed as an unbalanced of rotating elements (cage, balls or rollers). During the current studies, such a defect has been simulated in a rolling bearing by extracting one roller.

However, when a cage defect occurs usually is a result of the rolling bearing damage due to cage wearing or fracture of the cage material.

In the plot of Figure 11 can be seen the relationship between the shaft rotation speed, measured through a photoelectric cell, and the equivalent cage rotation speed, measured through the stroboscopic lamp, previously mentioned. The speed change of the cage rotation as a function of the shaft rotation (inner race) at constant load, allows the observation of the cage sliding

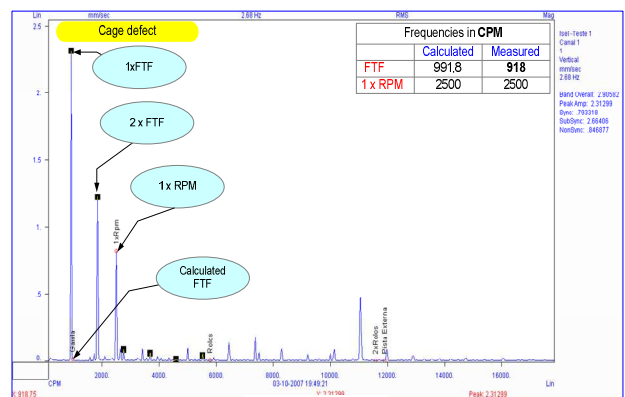


Fig. 10. Spectrum of speed [mm/s] – defect FTF.

phenomena.

However, the plot of Figure 11 should be analysed in relative terms, since an exaggerated sliding has been intentionally introduced for didactic purposes. This exaggerated value for the sliding is a consequence of the disrespect to the minimum radial load recommended by the rolling bearing makers for rolling bearings with cylindrical rolling elements, which has been used during the current studies.

The measured values for the defect frequencies are computed as a function of the cage rotation speed. However, the mathematical formulation expressed by equations (10), (13), (15) and (19) are a function of the rolling bearing geometric parameters. Therefore, the cage rotational speed impact on their values is hidden by the model, since the cage rotation speed does not appear explicitly in equations.

A detailed analysis of the spectrums presented above allows concluding that always exist a deviation between the values evaluated through the theoretical mathematical model and the values measured using the experimental setup. During the current studies has been observed that the factor responsible for that deviation is the cage rotation speed.

However, the mathematical formulation previous presented has been derived considering no sliding effect between the elements of the rolling bearing. This fact is illustrated with the plot of Figure 5, where the computed defect frequency (14551 CPM) is lower than the measured defect frequency (14973 CPM). The inner race rotation frequency is in this case 2004 CPM, while the cage rotation frequency is 753 CPM.

Although equation (15) does not easily allow justifying the referred deviation, if equation (14) is analysed careful the results look obvious, justifying the deviation and confirming the defect frequency corresponding to the fault above mentioned. Therefore, current studies allow concluding that, in the presence of sliding, the value measured for defect frequency considering a fault in the inner race of the rolling bearing is always higher than the values obtain using the theoretical mathematical models previously described.

Furthermore, the value for defect frequency of a fault in the outer race of a rolling bearing, when sliding is considered, is always lower than the corresponding values achieved using the theoretical models. In a similar way, the defect frequency for a fault in a roller of a rolling bearing, considering sliding, is always lower than the computed corresponding frequency.

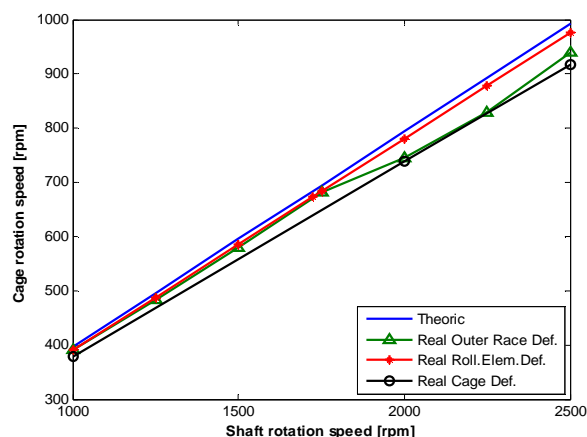


Fig. 11. Cage speed change at constant load.

7 Conclusions

Tests performed during the present study show the influence of the cage rotation speed in the emitted frequencies of a faulty rolling bearing. Such influence can not be seen by analysing the mathematical formulation used in the computation of the quoted defect frequencies. To simulate changes in the cage speed, a didactic approach has been followed in order to obtain an intentional exaggerated sliding to demonstrate its effect in the spectral analysis. We emphasize the application of the referred deviations between computed and measure data as an effective decision support tool. The use of rolling bearings with cylindrical roller elements, in tests conducted during the current studies, eliminate the influence of other geometric parameters, such as the contact angle. The influence of that parameter in fault diagnosis of faulty rolling bearings is under study and will be soon pointed out.

Acknowledgements:

Research for this paper was partially supported by Project POCTI-SFA-10-46-IDMEC of FCT, funded by POCI 2010, POSC, FSE and MCTES.

References:

- [1] T. Farinha, I. Fonseca and M. Barbosa, "New approaches on predictive maintenance based on a renewable perspective for wind generators", *New Aspects of Engineering Mechanics, Structures, Engineering Geology, Proceedings of the 1st WSEAS International Conference on Engineering Mechanics, Structures, and Engineering Geology (EMESEG'08)*, pp. 26-32, July 22-24 2008.

- [2] J. T. Leung and P. W. Tse, "Smart Asset Maintenance System for machine fault diagnosis - Its effectiveness, methodology, and applications", Proceedings of the IDET/CIE 2005, ASME 2005 International Design Engineering Technical Conferences & Computers and Information in Engineering Conference, Vol. 1, pp. 559-566, September 24-28 2005.
- [3] I. Fonseca, T. Farinha and M. Barbosa, "A computer system for predictive maintenance of wind generators", Proceedings of the 12th WSEAS International Conference on Computers, PTS 1-3 - New Aspects Of Computers, pp. 928-933, July 23-25 2008.
- [4] Jardine, A. K. S., Lin, D. and Banjevic, D., "A review of machinery diagnosis and prognostics implementing condition-based maintenance", Mechanical Systems and Signal Processing, 20, pp. 1483-1510, 2006.
- [5] Pan Y., Chen J. and Guo, L., "Robust bearing performance degradation assessment method based on improved wavelet packet-support vector data description", Mechanical Systems and Signal Processing, Vol. 23, No. 3, pp. 669-681, April 2009.
- [6] B. Tao, L. Zhu, H. Ding and Y. Xiong, "An alternative time-domain index for condition monitoring of rolling element bearing - A comparison study", Reliability Engineering & System Safety, Vol. 92, pp. 660-670, 2007.
- [7] S. Orhan, N. Akturk and V. Celik, "Vibration monitoring for defect diagnosis of element bearings as a predictive maintenance tool: Comprehensive case studies", NDT&E International, Vol. 39, pp. 293-298, 2006.
- [8] V. Sugumaran, V. Muralidharan and K. I. Ramachandra, "Feature selection using Decision Tree and classification through Proximal Support Vector Machine for fault diagnostics of roller bearing", Mech. Syst. Signal Proc., Vol. 21, pp. 930-942, 2007.
- [9] A. Repanovici, "Information Technology Implication in Student Behaviour for Information Literacy Skills", Proceedings of the 4th WSEAS/IASME International Conference on Educational Technologies (EDUTE'08), Corfu, Greece, pp. 81-86, October 26-28 2008.
- [10] V. Wowk, Machinery Vibration - Measurement and Analysis, McGraw-Hill, N. York, pp. 146-161, 1991.
- [11] J. Antoni, "Cyclic spectral analysis of rolling-element bearing signals: Facts and fictions", Journal of Sound and Vibration, Vol. 304, pp. 497-529, 2007.
- [12] N. Tandon, G.S. Yadava and K.M. Ramakrishna, "A comparison of some condition monitoring techniques for the detection of defect in induction motor ball bearings", Mechanical Systems and Signal Processing, Vol. 21, No. 1, pp. 244-256, January 2001.
- [13] H. Ocak and K.A. Loparo, "Estimation of the running speed and bearing defect frequencies of an induction motor from vibration data", Mechanical Systems and Signal Processing, Vol.18, No. 3, pp. 515-533, May 2004.
- [14] B. Li, M.-Y. Chow, Y. Tipsuwan and J.C. Hung, "Neural-network-based motor rolling bearing fault diagnosis", IEEE Transactions on Industrial Electronics, Vol. 47, No. 5, pp. 1060-1069, October 2000.
- [15] N. Tandon and A. Choudhury, "A review of vibration and acoustic measurement methods for the detection of defects in rolling element bearings", Tribology Internat., Vol. 32, No. 8, pp. 469-480, August 1999.
- [16] M. Xu, "Spike Energy and its applications", The Shock and Vibration Digest, Vol. 27, No. 3, pp. 11-17, May/June 1995.
- [17] O. J. L. Castro, C. C. Sisamon and J. C. G. Prada, "Bearing Fault Diagnosis based on Neural Network Classification and Wavelet Transform", Proceedings of the 6th WSEAS International Conference on Wavelet Analysis & Multirate Systems, Bucharest, Romania, pp. 22-29, October 16-18 2006.
- [18] H. Wang and P. Chen, "Fault Diagnosis for a Rolling Bearing Used in a Reciprocating Machine by Adaptive Filtering Technique and Fuzzy Neural Network", WSEAS Transactions on Systems, Issue 1, Volume 7, pp. 1-6, January 2008.
- [19] A. A. Roque, T. A. Silva, J. M. F. Calado and J. C. Q. Dias, "Rolling bearing fault detection and isolation - A didactic study", Proceedings of the 4th WSEAS/IASME International Conference on EDUCATIONAL TECHNOLOGIES (EDUTE'08), Corfu, Greece, pp. 132-137, October 26-28 2008.